CHEMISTRY
A EUROPEAN JOURNAL

DOI: 10.1002/chem.200501020

Mechanistic Studies of the Photocatalytic Oxidation of Trichloroethylene with Visible-Light-Driven N-Doped TiO_2 Photocatalysts

Soon-Kil Joung,* Takashi Amemiya, Masayuki Murabayashi, and Kiminori Itoh[a]

Abstract: Visible-light-driven TiO_2 photocatalysts doped with nitrogen have been prepared as powders and thin films in a cylindrical tubular furnace under a stream of ammonia gas. The photocatalysts thus obtained were found to have a band-gap energy of 2.95 eV. Electron spin resonance (ESR) under irradiation with visible light ($\lambda \geq 430$ nm) afforded the increase in intensity in the visible-light region. The concentration of trapped holes was about fourfold higher than that of trapped electrons. Nitrogen-doped TiO_2 has been used to investigate mechanistically the photocatalytic oxidation of trichloroethylene (TCE) under irradiation with visible light ($\lambda \geq 420$ nm). Cl and O radicals, which contribute significantly to the generation of dichloroacetyl chloride (DCAC) in the photocatalytic oxidation of TCE under UV irradiation, were found to be deactivated under irradiation with visible light. As the main by-product, only phosgene was detected in the photocatalytic oxidation of TCE under irradiation with visible light. Thus, the reaction mechanism of TCE photooxidation under irradiation with visible light clearly differs markedly from that under UV irradiation. Based on the results of the present study, we propose a new reaction mechanism and adsorbed species for the photocatalytic oxidation of TCE under irradiation with visible light. The energy band for TiO_2 by doping with nitrogen may involve an isolated band above the valence band.

Keywords: electronic structure · mechanistic studies · N-doped titania · photocatalysts · photooxidation · reaction mechanisms · titanium dioxide · trichloroethylene

Introduction

Ultraviolet (UV) photocatalysts have been developed and applied in the efficient use of solar light and in environmental cleaning on both local and global scales.[1–3] TiO_2, one of the best-known UV photocatalysts, has been widely used because of its lack of toxicity, relative inexpensiveness, high activity, and chemical stability.[4–6] In general, photocatalytic reactions are initiated by the generation of electron-hole pairs upon irradiation with UV light, the energy of which is greater than the band-gap energy for TiO_2 of 3.2 eV ($\lambda < 387$ nm).[7] However, these UV photocatalysts show poor absorption of visible light, which constitutes 45% of solar energy and 90% of indoor light, and can make use of only 3–4% of solar energy due to the large band-gap energy of 3.2 eV. Thus, a great deal of effort has been directed towards the development of visible-light-driven photocatalysts that can efficiently utilize solar and/or indoor light in the environmental and energy fields.[8–10] Several types of visible-light-driven photocatalysts have been developed. For example, Khan et al. reported a chemically modified (CM) *n*-TiO_2 synthesized by flame pyrolysis of Ti metal sheets.[11] Ohno et al. reported S-doped TiO_2, which adopted rutile and anatase structures under high- and low-temperatures, respectively.[9] Anpo et al. prepared second-generation TiO_2 photocatalysts by an advanced metal ion implantation method.[2,12] Kisch et al. reported amorphous microporous metal oxides of titanium (AMM-Ti) modified with platinum(IV) chloride (Pt^{IV}/AMM-Ti).[13] In addition, nitrogen-doped TiO_2 ($TiO_{2-X}N_X$), as reported by Sato[14] and Asahi et al.,[15] can be easily prepared and has therefore attracted a great deal of interest. Thus, there have been a number of studies regarding the preparation of $TiO_{2-X}N_X$[16,17] and its band-gap energy structure[8,16,18–21] associated with the response in the visible-light region. Models of the band-gap energies of $TiO_{2-X}N_X$ and raw, undoped TiO_2 are shown in Figure 1. Figure 1a shows the band-gap energy structure of the anatase-type UV-driven photocatalyst, while Figure 1b,

[a] Dr. S.-K. Joung, Prof. Dr. T. Amemiya, Prof. Dr. M. Murabayashi, Prof. Dr. K. Itoh
Graduate School of Environment and Information Sciences
Yokohama National University
79–7 Tokiwadai, Hodogaya-ku, Yokohama 240–8501 (Japan)
Fax: (+81) 45-339-4354
E-mail: joungskynu@yahoo.co.jp

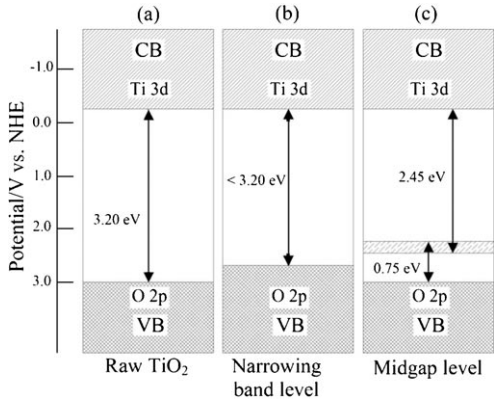

Figure 1. Models of the band-gap energy structures of $TiO_{2-X}N_X$ for responses in the visible-light region. See text for details.

reported by Asahi et al.,[15] shows the narrowed band-gap structure obtained by mixing of N 2p and O 2p orbitals. Figure 1c, reported by Nakamura et al.,[19] shows the midgap energy level formed slightly above the valence band. The schemes represented in Figure 1b and c are both used in engineering for visible-light-driven photocatalyst materials. Mechanisms to achieve responsiveness to visible light are still under investigation, and no complete interpretation has yet been formulated. Thus, the mechanisms of reactions of specific compounds (such as TCE) with $TiO_{2-X}N_X$ may help in delineating the mechanistic aspects of reactivity in the visible-light region.

The volatile chlorinated organic compound (VCOC) trichloroethylene (TCE; $CHClCCl_2$) has been used as an industrial solvent for degreasing and dry cleaning, and has become one of the most common environmental contaminants.[22–24] There have been a number of studies of the photocatalytic oxidation of TCE with TiO_2 under UV irradiation,[1,25,26] and a practical reaction plant has also been reported.[27] Cl and O radicals play important roles in the photocatalytic oxidation of TCE under UV irradiation, and contribute significantly to the generation of dichloroacetyl chloride (DCAC).[22,28–32] DCAC generated during the photocatalytic oxidation of TCE is converted into phosgene under UV irradiation.[28,31,32] The main gas-phase by-products/intermediates during the photocatalytic oxidation of TCE under UV irradiation are thus known to be DCAC and phosgene.[31] However, only DCAC is adsorbed on TiO_2.[4]

In the present study, we have photocatalytically oxidized trichloroethylene (TCE) under irradiation with visible light using N-doped TiO_2 photocatalysts, and have investigated the mechanisms that underpin the degradation reaction. In addition, we have also investigated the species adsorbed on TiO_2 during the photocatalytic oxidation of TCE with regard to the mechanisms involved.

Results

Preparation and characterization of N-doped TiO_2: In the case of Si-$TiO_{2-X}N_X$ films, the crystalline forms before and after doping with nitrogen were characterized as being of anatase-type, with a crystalline size of 11 nm.

Figure 2A shows a comparison of the UV/Vis diffuse reflectance spectra of $TiO_{2-X}N_X$ and undoped TiO_2. The prepared $TiO_{2-X}N_X$ photocatalysts, in the form of powders or thin films, were very vivid yellow in color, and showed a shift to longer wavelengths in accordance with color. Figure 2B shows plots of the modified Kubelka–Munk function versus the photon energy, from which the band-gap energies can be obtained.[33] The band-gap energy for $TiO_{2-X}N_X$ can be seen to be 2.95 eV, corresponding to the visible-light region, whereas that for undoped TiO_2 is 3.2 eV.

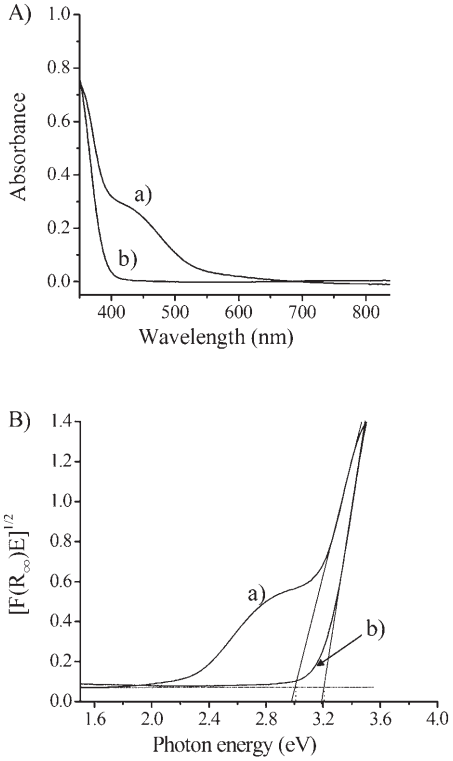

Figure 2. A): UV/Vis diffuse reflectance spectra of the samples. B): Plot of the modified Kubelka–Munk function versus the photon energy of the samples. a) After doping with nitrogen; b) commercial UV photocatalyst (ST-01). Doping conditions: 10 min at 873 K under a stream of ammonia gas.

While the N 1s X-ray photoelectron spectrum of $TiO_{2-X}N_X$ shown in Figure 3 features a peak at 399.95 eV, known to be attributable to adsorbed NO or N in Ti-O-N,[34] no weak peak attributable to Ti–N bonding can be seen at 396 eV due to the noise, as shown in the upper trace in Figure 3A. In the case of undoped TiO_2 powder, neither peak is observed, as shown in the lower trace in Figure 3A. Peaks for Ti $2p_{3/2}$ and Ti $2p_{1/2}$ observed at 458.6 eV and 464.3 eV (Figure 3B), respectively, are known to be due to Ti^{4+} in

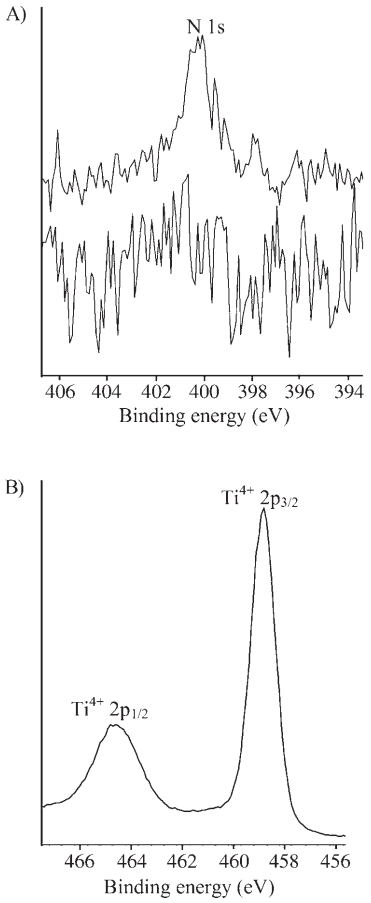

Figure 3. A): N 1s X-ray photoelectron spectra of $TiO_{2-X}N_X$ (upper trace) and TiO_2 powders (lower trace). B): X-ray photoelectron spectrum of Ti 2p peaks of $TiO_{2-X}N_X$ powders.

pure anatase titania form.[2] Sato et al. reported that the peak at 396 eV in the N 1s spectrum is directly associated with the formation of Ti–N bonding.[16] However, whether the peak at 399.95 eV in the N 1s spectrum of $TiO_{2-X}N_X$ is due to adsorbed NO or N in Ti-O-N is still under investigation. Although we tentatively assign the N 1s peak at 399.95 eV to N in Ti-O-N, based on the previous reports of Nakamura et al.[19] and Gole et al.[35] and the results of electron spin resonance (ESR) studies (Figure 4), it is our intention to investigate the assignment of peaks in the N 1s spectrum in detail in the near future. The ESR spectra shown in Figure 4 indicate changes in the intensities for $TiO_{2-X}N_X$ powders under irradiation with visible light ($\lambda \geq 430$ nm) and in the dark. The signals with g values of less than 2.0 are known to be due to trapped electrons,[36–39] while those with g values in the range from 2.00 to 2.03 are known to be due to trapped holes.[36–42] All signals intensified markedly upon irradiation with visible light, and the concentrations of the trapped holes were about fourfold higher than those of the trapped electrons. These spectra represent important results indicating the increased intensity in the visible-light region for $TiO_{2-X}N_X$. In addition, ESR measurements under irradiation with visible light revealed differences between

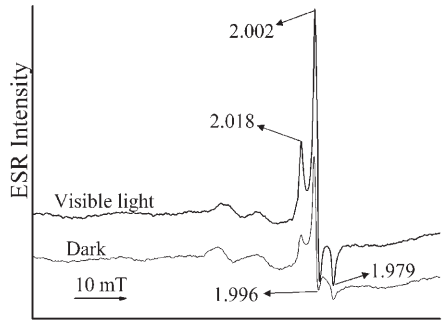

Figure 4. ESR spectra (gray) under visible light ($\lambda \geq 430$ nm) and (black) in the dark for $TiO_{2-X}N_X$ powders. Doping conditions: 10 min at 873 K under a stream of ammonia gas.

$TiO_{2-X}N_X$ and the undoped oxide upon the absorption of photons, such as the formation of electron-hole pairs.

Gas-phase products of the photocatalytic oxidation of TCE: The infrared absorption spectra shown in Figure 5 indicate the by-products and concentration changes during the course of photocatalytic oxidation of TCE (1.8×10^{-4} mol L^{-1}) with $TiO_{2-X}N_X$ powders under irradiation with visible light. The characteristic peaks in the TCE gas-phase spectrum (Figure 5a), appearing at 3170, 3100, 1595, 1560, 1254, 1246 (shoulder), 944, 848, and 780 cm^{-1}, disappeared completely after irradiation with visible light for 105 min (Figure 5d). New bands appeared due to gas-phase species such as phosgene ($COCl_2$), CO, and HCl during the photocatalytic oxidation of TCE under irradiation with visible light and the infrared absorbance intensity of CO_2 also in-

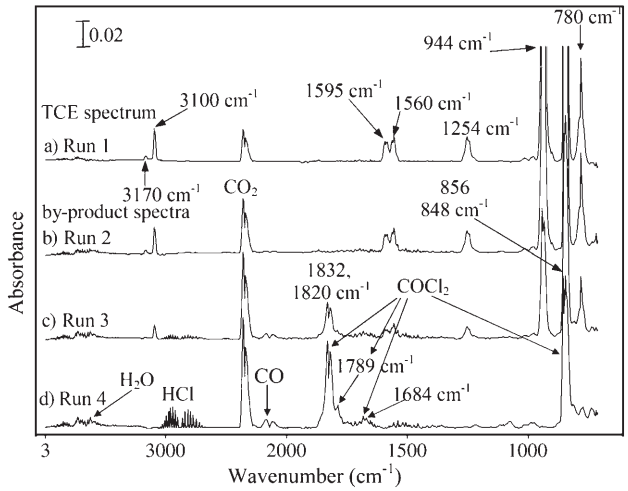

Figure 5. Infrared spectra of photocatalytic oxidation of TCE (1.8×10^{-4} mol L^{-1}) at different reaction times with $TiO_{2-X}N_X$ powders: a) gas-phase spectrum of TCE; b)–d) by-product spectra during photocatalytic degradation of TCE. Four successive experiments were carried out with the same $TiO_{2-X}N_X$ powders. The infrared bands are assigned to the following gas-phase photoproducts: $COCl_2$, CO, CO_2, and HCl, as shown in Table 1. The phosgene concentration generated in Figure 5d was 1.10×10^{-5} mol L^{-1}.

creased. Infrared bands due to phosgene (1.10×10^{-5} mol L^{-1}), the main by-product, were observed near 1832, 1820, 1789, 1684, 856, and 848 cm^{-1}, corresponding to those reported previously.[4] Bands due to HCl were observed between 3066 and 2675 cm^{-1}, and CO bands were observed at 2172 and 2115 cm^{-1}. However, DCAC, which was the major by-product observed in the photocatalytic oxidation of TCE under UV irradiation, was not observed.

On the other hand, the photoproducts of TCE photooxidation with visible-light-driven photocatalysts ($TiO_{2-X}N_X$) and with UV-driven photocatalysts under UV irradiation were the same, that is, DCAC and phosgene were the main intermediates. This indicates that the differences in the photoproducts observed between visible light and UV irradiation were due to the difference in photon energy.

The plots in Figure 6 show the changes in the concentrations of TCE and the by-products observed in the infrared spectra during photocatalytic oxidation of TCE at different

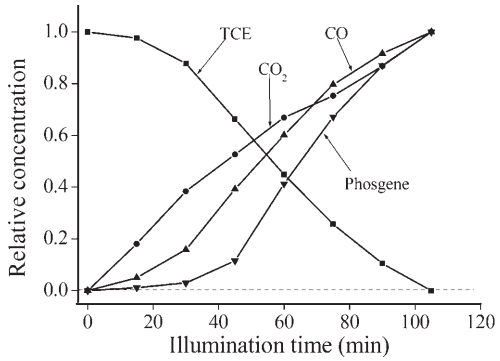

Figure 6. Changes in the concentrations of TCE and products at room temperature as a function of illumination time with visible light. These plots were obtained from the intensity changes in the infrared spectra and have been normalized for ease of comparison.

reaction times. These plots include only the main by-products and have been obtained from the intensities of the gas-phase infrared bands, specifically the bands at 944 cm^{-1} for TCE, 2360 cm^{-1} for CO_2, 2171 cm^{-1} for CO, and 1832 cm^{-1} for phosgene. Each plot has been normalized at the beginning or end of the reaction for ease of comparison. The curve for phosgene formation corresponds remarkably well to that for TCE consumption. This indicates that TCE photooxidation is closely associated with the formation of phosgene under irradiation with visible light, as reported previously for the formation of DCAC under UV irradiation.[22,32,43]

In Table 1, the gas-phase photoproducts of photocatalytic oxidation of TCE under UV irradiation and under irradiation with visible light, as detected by infrared spectroscopy, mass spectrometry, and the inspection tube method, are compared with results reported in the literature. Phosgene, which is formed from DCAC under UV irradiation,[25,31,32,44] and molecular chlorine (Cl_2) were observed under irradiation with visible light as well as UV. However, DCAC, the

Table 1. Gas-phase products of photocatalytic oxidation of TCE with different light sources and different analysis equipment in the present and previous studies.

		UV-BLB	Visible light ($\lambda \geq 420$ nm) (this work)
FT-IR	literature[a]	DCAC, $COCl_2$ CO, CO_2, HCl	not reported
	this work	DCAC, $COCl_2$ CO, CO_2, HCl	$COCl_2$, CO, CO_2, HCl
GC-MS	literature[b]	DCAC, $COCl_2$, HCl, Cl_2 CO_2, $CHCl_3$, CCl_4, C_2HCl_5, C_2Cl_4, C_2Cl_6	not reported
	this work	DCAC, $COCl_2$ CO_2, $CHCl_3$, C_2HCl_5	$COCl_2$, CO_2, $CHCl_3$, C_2HCl_5
inspection tube (this work)		Cl_2	Cl_2

[a] Ref. [45]. [b] Refs. [46–48].

major intermediate produced by the photocatalytic oxidation of TCE under UV irradiation, was not observed in either the FT-IR spectrum or the mass spectrum under irradiation with visible light. Thus, the mechanism of photodegradation of TCE under irradiation with visible light is probably different from that under UV irradiation.

Species adsorbed on TiO_2 during photocatalytic oxidation: DCAC and phosgene have been reported to be the species adsorbed on the surface of TiO_2 during photocatalytic oxidation of TCE under UV irradiation.[31] Previously, we reported that only DCAC was adsorbed on the TiO_2 during this process; the adsorbed DCAC is subsequently converted to adsorbed phosgene by photooxidation under UV irradiation.[4]

On the other hand, the results described in the previous section indicate that phosgene was the major by-product during photocatalytic oxidation of TCE under irradiation with visible light. As the photocatalytic reaction occurs on the surface of TiO_2, we investigated the species adsorbed on the surface of TiO_2 during the photooxidation of TCE to determine the mechanism of its photodegradation. To this end, photocatalytic oxidation of TCE was performed using thin films of Si-$TiO_{2-X}N_X$ under irradiation with visible light.

The infrared spectra in Figure 7 show the results of the photocatalytic oxidation of TCE using thin films of Si-$TiO_{2-X}N_X$ to investigate the species adsorbed on TiO_2. As shown in Figure 7b, $COCl_2$, CO, CO_2, H_2O, and HCl as gas-phase and adsorbed species were observed during the photocatalytic oxidation of TCE (Figure 7a) under irradiation with visible light. The observed by-products are the same as those observed during photocatalytic oxidation of TCE with $TiO_{2-X}N_X$ powders. After removal of the gas-phase species from within the infrared cell by purging with dry air or N_2, only an adsorbed species giving rise to bands at 1608 and 1238 cm^{-1} remained as the main surface species, as detected by in situ FT-IR spectroscopy (Figure 7c), which corresponds to standard adsorbed phosgene as shown in the

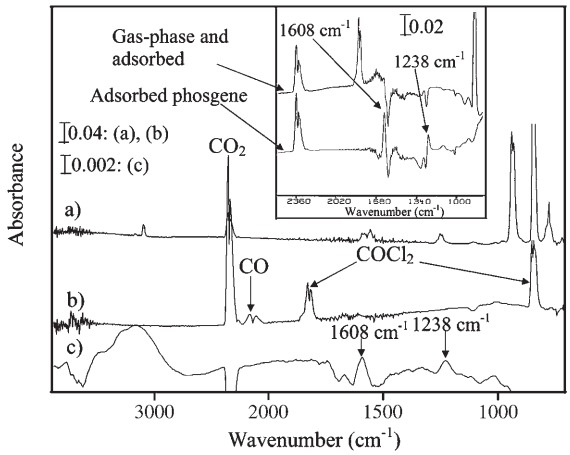

Figure 7. Infrared spectra of photocatalytic oxidation of TCE with thin films of Si-$TiO_{2-X}N_X$: a) spectrum of gas-phase and adsorbed starting TCE; b) spectrum of gas-phase and adsorbed product species during photocatalytic oxidation of TCE; c) spectrum of only adsorbed species after removal of the gas-phase species with dry air under the conditions shown in (b). The infrared bands of adsorbed species following photooxidation of TCE in (c) are assigned to adsorbed phosgene. The inset shows the infrared spectra of (top) gas-phase and adsorbed phosgene and (bottom) adsorbed phosgene alone. The relative humidity during acquisition of spectrum (b) was about 2.1%.

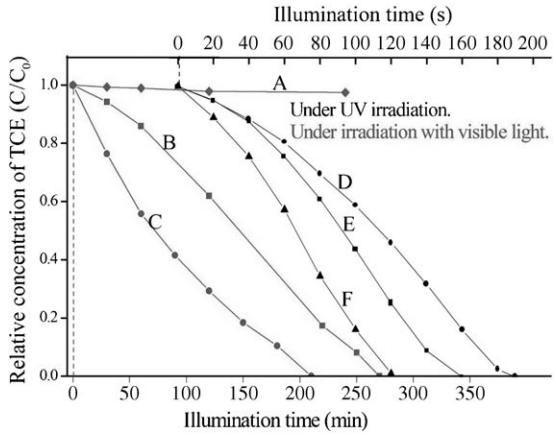

Figure 8. Changes in the concentration of TCE by photocatalytic oxidation with different adsorbed species under irradiation with visible light and under UV irradiation (initial concentration of TCE 3.6×10^{-4} mol L^{-1}). Under visible light: A) control (TCE photooxidation using a commercial UV-photocatalyst), B) without adsorbed species (initial photocatalytic oxidation of TCE), C) with adsorbed phosgene. Under UV: D) with adsorbed DCAC, E) without adsorbed species (initial photocatalytic oxidation of TCE), F) with adsorbed phosgene. The introduced concentrations for adsorption were DCAC 6.67×10^{-5} mol L^{-1} and phosgene 2.22×10^{-5} mol L^{-1}).

lower trace of the inset in Figure 7. No significant changes, such as a band shift or the appearance of a new band in the infrared spectrum, were observed on using different purging gases, that is, dry air or N_2. Likewise, the use of BaF_2 windows had no effect on the detection of adsorbed species after the removal of gas-phase species by purging with dry air or N_2. Therefore, the species adsorbed on TiO_2 during the photooxidation of TCE under irradiation with visible light was considered to be phosgene.

In our previous study, we showed that gas-phase phosgene accelerates the photocatalytic oxidation of TCE and volatile non-chlorinated organic compounds under UV irradiation due to chlorine radicals dissociated from molecular Cl_2 and phosgene.[22] Therefore, we examined the effect of adsorbed phosgene on the photocatalytic oxidation of TCE using thin films (Si-$TiO_{2-X}N_X$ and Si-TiO_2) under irradiation with visible light and under UV irradiation. The plots in Figure 8 show the changes in the concentration of TCE on the TiO_2 surface upon its photocatalytic oxidation (starting concentration 3.6×10^{-4} mol L^{-1}) in the presence of adsorbed phosgene (introduced concentration for adsorption: 2.22×10^{-5} mol L^{-1}) or adsorbed DCAC (introduced concentration for adsorption: 6.67×10^{-5} mol L^{-1}) under UV irradiation and in the presence of adsorbed phosgene under irradiation with visible light. Line A in Figure 8 shows the photooxidation of TCE with commercial UV photocatalysts under irradiation with visible light. Lines B and E indicate standard photocatalytic oxidations of TCE without the adsorbed species under visible light and under UV irradiation, respectively. While adsorbed DCAC on the TiO_2 surface did not accelerate the degradation of TCE under UV irradiation, as shown by line D, adsorbed phosgene accelerated the degradation reaction, as shown by lines F and C, with apparent quantum yield ratios of about 1.3 in both cases, compared to lines E and B, respectively. These results indicate that phosgene adsorbed on TiO_2 accelerates the photocatalytic oxidation of TCE under irradiation with visible light as well as under UV irradiation. The apparent quantum yield ratio between UV and visible light activation in the photocatalytic oxidation of TCE was about 176 (Figure 8). In analysis of the XPS data (Table 2), although the relative amount of chlorine in the adsorbed phosgene is only a quarter of that in the adsorbed DCAC, the decrease in TCE concentration is faster with adsorbed phosgene than with adsorbed DCAC. Therefore, we conclude that, apart from Cl radicals, active species that accelerate the degradation reaction of TCE stem from the adsorbed phosgene. Further detailed studies are required to fully characterize the active species involved under irradiation with visible light.

Table 2. Results of quantitative analysis of species adsorbed on the TiO_2 surface by XPS.

Analyzed samples	Analyzed elements [%]		
	C 1s	O 1s	Cl 2p
standard adsorbed DCAC	16.1	80.1	3.7
adsorbed DCAC produced from photocatalytic oxidation of TCE under UV-BLB	13.4	82.7	4
standard adsorbed phosgene	9.5	89.6	0.95

Discussion

The role of oxygen radicals (·O) and Cl radicals (·Cl) in the photocatalytic oxidation of TCE under UV irradiation: Electron-hole pairs are generated by excitation when the surface of TiO_2 is irradiated with photons [Eq. (1)]. Subsequently, the hole (h^+) and the electron (e^-) oxidize and reduce chemical species, such as OH groups and oxygen, respectively, on the surface of the TiO_2 [Eqs. (2) and (3); VB = valence band; CB = conduction band]. Surface reactions with holes and electrons form OH radicals and superoxide ions (O_2^-),[23,34] and the latter subsequently react with holes to form oxygen radicals (·O) [Eq. (4)].[49]

$$TiO_2 \overset{h\nu}{\rightleftharpoons} h^+(VB) + e^-(CB) \quad (1)$$

$$h^+(VB) + OH^- \rightarrow {}^{\cdot}OH \text{ (oxidation reaction)} \quad (2)$$

$$e^-(CB) + O_2 \rightarrow O_2^- \text{ (reduction reaction)} \quad (3)$$

$$h^+(VB) + O_2^- \rightarrow 2\,{}^{\cdot}O \text{ (oxidation reaction)} \quad (4)$$

The O radicals initiate the oxidation reaction of TCE on the TiO_2 surface, as shown in Equations (5) and (6).[31] Under UV irradiation, the subsequent reactions produce by-products, principally phosgene and DCAC.

$$C_2HCl_3 \text{ (TCE)} + O_2 \xrightarrow[TiO_2]{UV} {}^{\cdot}C_2HCl_3O + {}^{\cdot}O \quad (5)$$

$$\begin{aligned} {}^{\cdot}C_2HCl_3O \rightarrow {} & COCl_2 \text{ (phosgene)} + CHCl_2CClO \text{ (DCAC)} \\ & + CO + CO_2 + HCl + CHCl_3 + C_2HCl_5 \end{aligned} \quad (6)$$

Under UV irradiation, molecular chlorine (Cl_2), generated by several pathways in the decomposition of TCE, undergoes repeated photolysis and formation, as shown in Equation (7).[22,50,51] The Cl radicals thus formed initiate a chain reaction, and produce DCAC from the decomposition reaction of TCE under UV irradiation as sown in Equations (7)–(11).[22,28,29]

$$Cl_2 \overset{h\nu}{\rightleftharpoons} 2\,{}^{\cdot}Cl \quad (7)$$

$$CCl_2CHCl \text{ (TCE)} + {}^{\cdot}Cl \rightarrow {}^{\cdot}CCl_2CHCl_2 \quad (8)$$

$${}^{\cdot}CCl_2CHCl_2 + O_2 \rightarrow {}^{\cdot}OOCCl_2CHCl_2 \quad (9)$$

$${}^{\cdot}OOCCl_2CHCl_2 \rightarrow {}^{\cdot}OCCl_2CHCl_2 + {}^1\!/_2O_2 \quad (10)$$

$${}^{\cdot}OCCl_2CHCl_2 \rightarrow CHCl_2COCl \text{ (DCAC)} + {}^{\cdot}Cl \quad (11)$$

The DCAC produced from the reactions in Equations (7)–(11) generates phosgene as the major by-product by way of the reactions given in Equations (12)–(15).[22,25]

$$CHCl_2COCl \text{ (DCAC)} + {}^{\cdot}OH \rightarrow {}^{\cdot}CCl_2COCl + H_2O \quad (12)$$

$${}^{\cdot}CCl_2COCl + O_2 \rightarrow {}^{\cdot}OOCCl_2COCl \quad (13)$$

$${}^{\cdot}OOCCl_2COCl \rightarrow {}^{\cdot}OCCl_2COCl + {}^1\!/_2O_2 \quad (14)$$

$${}^{\cdot}OCCl_2COCl \rightarrow COCl_2 \text{ (phosgene)} + {}^{\cdot}COCl \quad (15)$$

$${}^{\cdot}COCl \rightarrow CO + {}^{\cdot}Cl \quad (16)$$

Consequently, in the photocatalytic oxidation under UV irradiation, TCE is converted to DCAC, and this, in turn, is subsequently converted to phosgene. O radicals formed by reaction with holes and Cl radicals generated by photon energies in excess of about 3.2 eV play important roles in the above mechanisms for the formation of phosgene and DCAC. OH radicals also contribute to the formation of phosgene by way of Equations (12)–(15).

Proposed mechanism for photocatalytic oxidation of TCE with $TiO_{2-X}N_X$ under irradiation with visible light: The OH radicals photogenerated according to Equation (2) initiate the oxidation of TCE on the TiO_2 surface under UV irradiation [Eq. (17)], which, in turn, leads to subsequent reactions that produce OCClCHClOH and Cl radicals [Eqs. (18)–(20)].[25,44] These reaction processes are considered to be the same under irradiation with visible light.

$$CCl_2CHCl \text{ (TCE)} + {}^{\cdot}OH \rightarrow {}^{\cdot}CCl_2CHClOH \quad (17)$$

$${}^{\cdot}CCl_2CHClOH + O_2 \rightarrow {}^{\cdot}OOCCl_2CHClOH \quad (18)$$

$${}^{\cdot}OOCCl_2CHClOH \rightarrow {}^{\cdot}OCCl_2CHClOH + {}^1\!/_2O_2 \quad (19)$$

$${}^{\cdot}OCCl_2CHClOH \rightarrow OCClCHClOH + {}^{\cdot}Cl \quad (20)$$

The Cl radicals generated according to Equation (20) are deactivated in the photooxidation of TCE under irradiation with visible light, as are the O radicals, because DCAC is not detected under these conditions, as shown in Table 1. The Cl radicals are converted to molecular chlorine (Cl_2) according to Equation (7), because the rate of formation of molecular Cl_2 from Cl radicals is much faster (by a factor of 3.8×10^{21}) than the rate of the reverse reaction generating Cl radicals ($k_{Cl_2} = 3.1\times10^{11}\,cm^3\,mol^{-1}\,s^{-1}$, $k_{TCE} = 8.1\times10^{-11}\,cm^3\,mol^{-1}\,s^{-1}$).[29,52] The O radicals are likewise converted to molecular O_2.

In addition, the OCClCHClOH generated from reaction according to Equation (20) subsequently reacts with OH radicals under irradiation with visible light, because OH radicals have very strong oxidizing ability. We thus propose the following reaction mechanism [Eqs. (21)–(25)] for the generation of phosgene, the main by-product, under irradiation with visible light.

$$OCClCHClOH + {}^{\cdot}OH \rightarrow {}^{\cdot}CClOHCOCl + H_2O \quad (21)$$

$${}^{\cdot}CClOHCOCl + O_2 \rightarrow {}^{\cdot}OOCClOHCOCl \quad (22)$$

$${}^{\cdot}OOCClOHCOCl \rightarrow {}^{\cdot}OCClOHCOCl + {}^1\!/_2O_2 \quad (23)$$

$${}^{\cdot}OCClOHCOCl \rightarrow {}^{\cdot}COOH + COCl_2 \text{ (phosgene)} \quad (24)$$

$${}^{\cdot}COOH \rightarrow CO_2 + {}^{\cdot}H \quad (25)$$

The gas-phase phosgene, the major by-product, becomes adsorbed on the TiO_2 surface. Although the H radical is a well-known free radical,[53] further studies are required to clearly delineate the role of H radicals in the photocatalytic oxidation of TCE under irradiation with visible light. The mechanisms responsible for other by-products, such as $CHCl_3$ and C_2HCl_5, will also be investigated in future studies.

Structures of adsorbed species on the TiO_2 surface: Several types of structures for adsorbates on the surfaces of metal compounds have been reported.[54–57] With regard to the surface structures **I** and **II**, Hair reported that structure **II** gives

I II

rise to bands at 1630 and 1220 cm^{-1}, while structure **I** yields bands at 1570 and 1330 cm^{-1} due to a splitting of degenerate vibrations.[54] Moreover, the difference in the COO vibrational frequencies, $\Delta\nu = (\nu_{as} - \nu_s)$, gives an indication of stability. That is to say, stronger bonds are associated with greater $\Delta\nu$ values.[55] As shown in Figure 7c, bands due to an adsorbed species are observed at 1608 and 1238 cm^{-1} during the photocatalytic oxidation of TCE under irradiation with visible light, which can be assigned to the COO asymmetric stretching vibration and the COO symmetric stretching vibration, respectively.[4]

The species obtained upon adsorption of phosgene was seen to be stable during photocatalytic reaction for 120 min under UV irradiation or during heating for 60 min at 473 K in air. Thus, we consider phosgene to be strongly adsorbed by reaction with water or OH groups on the TiO_2 surface (structure **III**), which is at variance with a previous report that chemical adsorption was temperature-dependent.[58] The surface of TiO_2 usually bears chemically or physically adsorbed hydroxyl groups or water, as shown in structure **III**.[34] Gas-phase H_2O and adsorbed OH groups are strongly linked with the photocatalytic activity. Amama et al. of our research group reported that humidity decreased the photocatalytic activity in the photocatalytic oxidation of TCE.[23] Equation (26) shows the process of adsorption of phosgene onto the TiO_2 surface.

Furthermore, while carboxylate compounds on the surface reduce the photooxidation rate,[59] the rate of photocatalytic oxidation in the presence of adsorbed phosgene is accelerated, as in activation by bidentate carbonate compounds.[4] Thus, adsorbed phosgene on the TiO_2 surface is suggested to be in the form of a bidentate carbonate compound, as shown by structure **IV**. This structure may serve to improve the photocatalyst surface with regard to enhancing photocatalytic activity under irradiation with visible light as well as under UV irradiation.

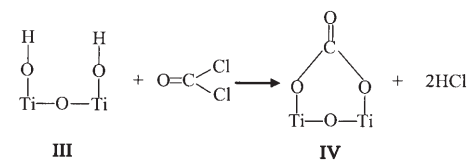

III IV

Mechanisms of reactivity of $TiO_{2-X}N_X$ in the visible-light region: The band-gap energy of the nitrogen-doped TiO_2 was found to be 2.95 eV, as mentioned in the relevant section above. The changes in intensity under irradiation with visible light was measured by ESR spectroscopy. The Cl and O radicals may be deactivated by photon energies over 3.2 eV, because DCAC was not generated during the photocatalytic oxidation of TCE with $TiO_{2-X}N_X$. The OH radicals were activated at band-gap energies of both 3.2 eV and 2.95 eV. Thus, the energy band for TiO_2 may not be narrowed upon doping with nitrogen, but may involve an isolated band above the valence band, as shown in Figure 9.

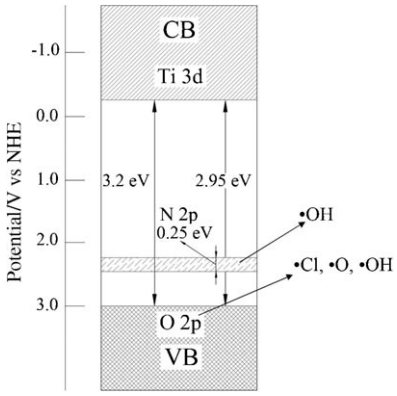

Figure 9. Schematic band structure for N-doped TiO_2 (anatase) prepared in the present study and radicals activated in each energy level by absorption of photon energy. VB: valence band; CB: conduction band.

Experimental Section

Materials: Trichloroethylene (TCE, 99.5%) and ammonia solution (NH_3, 28%) were purchased from Junsei Chemical Co., Ltd. (Tokyo, Japan). For the preparation of the sol, titanium(IV) isopropoxide (98%), absolute ethanol, and HCl were also purchased from Junsei Chemical Co., Ltd. (Tokyo, Japan). TiO_2 powder (ST-01) and the sol (STS-01) used in the thin film (Si-TiO_2), a commercial UV photocatalyst, were obtained from Ishihara Sangyo Kaisha, Ltd. (Tokyo, Japan) in the anatase crystalline form. Dry air or N_2 (ultra-high purity, 99.9995%) was used to remove gas-phase species from within an infrared cell.

Preparation and characterization of N-doped visible-light-driven TiO_2 photocatalysts: To analyze gas-phase species, TiO_2 powders were prepared as starting materials by evaporation of the volatiles from the sol prepared from titanium(IV) isopropoxide. Doping with nitrogen so as to obtain visible light-driven TiO_2 photocatalysts ($TiO_{2-X}N_X$) was performed under a flow of ammonia for 10 min at 873 K in a cylindrical tubular furnace.

Thin films on silicon wafers (Si-$TiO_{2-X}N_X$) were prepared to perform reactions aimed at identifying the species adsorbed on the surface of the

TiO_2. Silicon wafers were dipped into the sol prepared from titanium(IV) isopropoxide, and then exposed to a stream of NH_3 for 5 min at 773 K in a cylindrical tubular furnace.

Crystalline forms were ascertained by X-ray diffraction analysis (XRD; Rigaku, Tokyo, Japan) before and after nitrogen doping. The optical properties of the samples were measured with a UV/Vis spectrophotometer (JASCO, Tokyo, Japan). X-ray photoelectron spectroscopy (XPS) was used to characterize TiO_2 surfaces doped and undoped with nitrogen. Electron spin resonance (ESR; JEOL, Tokyo, Japan) was used to measure the changes in intensity and the extent of electron-hole pair formation under irradiation with visible light ($\lambda \geq 430$ nm; 500 W Hg lamp, USH-500 D); UV light was prevented from reaching the sample by means of a colored glass filter (Y-43, Toshiba, Shizuoka, Japan).

Photocatalytic oxidation of TCE and analysis of the photoproducts obtained from surface species: The cell used in the IR measurements consisted of a cylindrical Pyrex glass batchwise reactor (60.5 mL) with IR-transparent BaF_2 windows at both ends. The visible-light-driven TiO_2 photocatalysts and UV-driven TiO_2 photocatalysts (ST-01) were used in powder form to analyze the gas-phase photoproducts, while silicon wafers coated with TiO_2 (Si-$TiO_{2-X}N_X$, Si-TiO_2) were used to study the reactions involving the adsorbed species.

The visible-light source used was an HQI-TS/D250 W (total visible light intensity = 5.6 mW cm^{-2}; Toshiba, Tokyo, Japan); an optical high-path filter ($\lambda \geq 420$ nm; Fuji Film, Tokyo, Japan) was used to cut out UV light. The UV source used as a reference consisted of eight fluorescent black light blue lamps (UV-BLB; total intensity = 3.8 mW cm^{-2}, FL20S.BLB, Toshiba, Tokyo, Japan) with a peak wavelength of 352 nm (300–425 nm).

The gas-phase photoproducts formed during the photocatalytic oxidation of TCE were analyzed by FT-IR spectroscopy (Perkin-Elmer Spectrum GX FT-IR system; Nicolet 800 FT-IR spectrometer) and by gas chromatography-mass spectrometry (GC/MS; Hewlett Packard 6890/5973, Hewlett Packard, Palo Alto, CA). An inspection tube (Gastec, Kanagawa, Japan) was used to measure molecular chlorine (Cl_2). Adsorbed species on the surface of TiO_2 (Si-$TiO_{2-X}N_X$) were analyzed by means of in situ FT-IR measurements after removal of the gas-phase species by purging with dry air or N_2. In addition, XPS was used for a quantitative analysis of the adsorbate on the TiO_2 after analysis of the surface species by FT-IR.

Acknowledgements

The authors thank Mr. M. Kondo of the Instrumental Analysis Center, Yokohama National University, and Mr. F. Sakamoto of Thermo Electron K. K. for help with the XPS measurements. The authors would also like to thank Prof. Mikio Yagi, Yokohama National University, for help with the ESR measurements.

[1] J. Kim, K. Itoh, M. Murabayashi, *Denki Kagaku* **1996**, *64*, 1200–1202.
[2] M. Anpo, M. Takeuchi, *Int. J. Photoenergy* **2001**, *3*, 89–94.
[3] Y. Suda, H. Kawasaki, T. Ueda, T. Ohshima, *Thin Solid Films* **2004**, *453–454*, 162–166.
[4] S.-K. Joung, T. Amemiya, M. Murabayashi, K. Itoh, *Surf. Sci.*, in press.
[5] K. Hashimoto, T. Watanabe, K. Ishibashi, in *Photocatalysis: Science and Technology* (Eds.: M. Kaneko, I. Okura), Kodansha, Tokyo, **2002**, pp. 109–121.
[6] Y. Xie, C. Yuan, *Appl. Surf. Sci.* **2004**, *221*, 17–24.
[7] T. Tachikawa, S. Tojo, M. Fujitsuka, T. Majima, *J. Phys. Chem. B* **2004**, *108*, 11054–11061.
[8] T. Ihara, M. Miyoshi, Y. Iriyama, O. Matsumoto, S. Sugihara, *Appl. Catal. B: Environ.* **2003**, *42*, 403–409.
[9] T. Ohno, M. Akiyoshi, T. Umebayashi, K. Asai, T. Mitsui, M. Matsumura, *Appl. Catal. A* **2004**, *265*, 115–121.
[10] I. Tsuji, H. Kato, H. Kobayashi, A. Kudo, *J. Am. Chem. Soc.* **2004**, *126*, 13406–13413.
[11] S. U. M. Khan, M. Al-Shahry, W. B. Ingler, Jr., *Science* **2002**, *297*, 2243–2245.
[12] M. Anpo in *Photocatalysis: Science and Technology* (Eds.: M. Kaneko, I. Okura), Kodansha, Tokyo, **2002**, pp. 175–182.
[13] L. Zang, C. Lange, I. Abraham, S. Storck, W. F. Maier, H. Kisch, *J. Phys. Chem. B* **1998**, *102*, 10765–10771.
[14] S. Sato, *Chem. Phys. Lett.* **1986**, *123*, 126–128.
[15] R. Asahi, T. Morikawa, T. Ohwaki, K. Aoki, Y. Taga, *Science* **2001**, *293*, 269–271.
[16] S. Sato, R. Nakamura, S. Abe, *Appl. Catal. A* **2005**, *284*, 131–137.
[17] M.-C. Yang, T.-S. Yang, M.-S. Wong, *Thin Solid Films* **2004**, *469–470*, 1–5.
[18] H. Irie, Y. Watanabe, K. Hashimoto, *J. Phys. Chem. B* **2003**, *107*, 5483–5486.
[19] R. Nakamura, T. Tanaka, Y. Nakato, *J. Phys. Chem. B* **2004**, *108*, 10617–10620.
[20] Y. Sakatani, J. Nunoshige, H. Ando, K. Okusako, H. Koike, T. Takata, J. N. Kondo, M. Hara, K. Domen, *Chem. Lett.* **2003**, *32*, 1156–1157.
[21] O. Diwald, T. L. Thompson, T. Zubkov, E. G. Goralski, S. D. Walck, J. T. Yates, Jr., *J. Phys. Chem. B* **2004**, *108*, 6004–6008.
[22] a) L.-H. Zhao, S. Ozaki, K. Itoh, M. Murabayashi, *Electrochemistry* **2002**, *70*, 8–12; b) L.-H. Zhao, S. Ozaki, K. Itoh, M. Murabayashi, *Electrochemistry* **2002**, *70*, 171–173 [in Japanese].
[23] P. B. Amama, K. Itoh, M. Murabayashi, *J. Mol. Catal. B J. Mol. Catal. A* **2001**, *176*, 165–172.
[24] H.-J. Nam, T. Amemiya, M. Murabayashi, K. Itoh, *J. Phys. Chem. B* **2004**, *108*, 8254–8259.
[25] M. R. Nimlos, W. A. Jacoby, D. M. Blake, T. A. Milne, *Environ. Sci. Technol.* **1993**, *27*, 732–740.
[26] L. A. Dibble, G. B. Raupp, *Catal. Lett.* **1990**, *4*, 345–354.
[27] a) M. Murabayashi, *Anzen Kogaku* **2001**, *40*, 395–400 [in Japanese]; b) M. Murabayashi, *Ceramics Japan* **2004**, *39*, 515–518 [in Japanese].
[28] M. R. Nimlos, W. A. Jacoby, D. M. Blake, T. A. Milne in *Photocatalytic Purification and Treatment of Water and Air* (Eds.: D. F. Ollis, H. Al-Ekabi), Elsevier Science Publisher, New York, **1993**, pp. 387–392.
[29] a) P. G. Blystone, M. D. Johnson, W. R. Haag in *Air and Waste Management Association, 85th Annual Meeting*, June 21st, **1992**, Kansas City, MO; b) P. G. Blystone, M. D. Johnson, W. R. Haag, P. F. Daley in *Emerging Technologies In Hazardous Waste Management III* (Eds.: D. W. Tedder, F. G. Pohland), ACS Symposium Series, 518, American Chemical Society, Washington, DC, **1993**, pp. 380–392.
[30] L. Bertrand, J. A. Franklin, P. Goldfinger, G. Huybrechts, *J. Phys. Chem.* **1968**, *72*, 3926–3928.
[31] M. D. Driessen, A. L. Goodman, T. M. Miller, G. A. Zaharias, V. H. Grassian, *J. Phys. Chem. A* **1998**, *102*, 549–556.
[32] J. Fan, J. T. Yates, Jr., *J. Am. Chem. Soc.* **1996**, *118*, 4686–4692.
[33] B. Karvaly, I. Hevesi, *Z. Naturforsch. Teil A* **1971**, *26*, 245–249.
[34] A. L. Linsebigler, G. Lu, J. T. Yates, Jr., *Chem. Rev.* **1995**, *95*, 735–758.
[35] J. L. Gole, J. D. Stout, *J. Phys. Chem. A* **2004**, *108,* 1230–1240.
[36] Y. Nosaka in *Photocatalysis: Science and Technology* (Eds.: M. Kaneko, I. Okura), Kodansha, Tokyo, **2002**, pp. 69–85.
[37] Y. Nosaka, A. Nosaka, *Nyumon Hikari Shokubai*, Tokyo Tosho, Tokyo, **2004**, p. 72 (in Japanese).
[38] Y. Nakaoka, Y. Nosaka, *J. Photochem. Photobiol. A* **1997**, *110*, 299–305.
[39] J. M. Coronado, A. J. Maira, J. C. Conesa, K. L. Yeung, V. Augugliaro, J. Soria, *Langmuir* **2001**, *17*, 5368–5374.
[40] R. F. Howe, M. Grätzel, *J. Phys. Chem.* **1987**, *91*, 3906–3909.
[41] O. I. Micic, Y. Zhang, K. R. Cromack, A. D. Trifunac, M. C. Thurnauer, *J. Phys. Chem.* **1993**, *97*, 7277–7283.
[42] A. R. González-Elipe, J. Soria, G. Munuera, *Chem. Phys. Lett.* **1978**, *57*, 265–268.

[43] S.-J. Hwang, C. Petucci, C. Raftery, *J. Am. Chem. Soc.* **1997**, *119*, 7877–7878.
[44] K.-H. Wang, J.-M. Jehng, Y.-H. Hsieh, C.-Y. Chang, *J. Hazard. Mater.* **2002**, *B90*, 63–75.
[45] W. A. Jacoby, M. R. Nimlos, D. M. Blake, R. D. Noble, C. A. Koval, *Environ. Sci. Technol. Libr.* **1994**, *28*, 1661–1668.
[46] S. Kutsuna, Y. Ebihara, K. Nakamura, T. Ibusuki, *Atmos. Environ. A* **1993**, *27*, 599–604.
[47] W. F. Jardim, R. M. Alberici, M. K. Takiyama, C. P. Huang in *Proceedings of 26th Mid-Atlantic Industrial Waste Conference, Lancaster, PA*, **1994**, p. 230.
[48] C. H. Hung, B. J. Marinas, *Environ. Sci. Technol.* **1997**, *31*, 1440–1445.
[49] M. Formenti, S. J. Teichner, *Catalysis* **1979**, *2*, 87–106.
[50] H. Wang, T. O. Hahn, C. J. Sung, C. K. Law, *Combust. Flame* **1996**, *105*, 291–307.
[51] W.-P. Ho, R. B. Barat, J. W. Bozzelli, *Combust. Flame* **1992**, *88*, 265–295.
[52] S. Yamamoto, Ph. D. Thesis, Graduate School of Environment and Information Sciences, Yokohama National University, **2004**, p. 153 (in Japanese).
[53] M. Iwata, E. Takeshita, *Chemistry of the Environment*, JSSP, Tokyo, **2000**, p. 121 (in Japanese).
[54] M. L. Hair, *Infrared Spectroscopy in Surface Chemistry*, Marcel Dekker, New York, **1967**, p. 204.
[55] A. A. Davydov, *Infrared Spectroscopy of Adsorbed Species on the Surface of Transition Metal Oxides*, Wiley, Chichester, **1990**, p. 26.
[56] L. H. Little, *Infrared Spectra of Adsorbed Species*, Academic Press, London, New York, **1966**, p. 47.
[57] K. Nakamoto, *Infrared Spectra of Inorganic and Coordination Compounds*, Wiley, New York, **1963**, p. 197.
[58] A. Y. Nosaka, T. Fujiwara, H. Yagi, H. Akutsu, Y. Nosaka, *Langmuir* **2003**, *19*, 1935–1937.
[59] D. V. Kozlov, E. A. Paukshtis, E. N. Savinov, *Appl. Catal. B* **2000**, *24*, L7–L12.

Received: August 22, 2005
Revised: November 24, 2005
Published online: March 20, 2006

